# PARAMETER OPTIMIZATION OF ANTI-CRYSTALLIZATION FLOCKING DRAINAGE PIPE BASED ON MACRO FORCE AND DISPLACEMENT CHARACTERISTICS OF VILLUS

by

***Shiyang LIU[a*], Xuefu ZHANG[a,b], Feng GAO[a,b], Yun LI[a], and Saeed Hameed Kurdi AL DULAIMI[c]***

[a]College of Civil Engineering, Chongqing Jiaotong University, Chongqing, China
[b]State Key Laboratory of Mountain Bridge and Tunnel Engineering, Chongqing, China
[c]Department of Business Administration, Applied Science University, Kingdom of Bahrain

Original scientific paper
https://doi.org/10.2298/TSCI2106127L

*The crystal blockage of tunnel drainage pipe seriously affects the smoothness of the whole drainage system. Therefore, it is very important to effectively prevent crystal plugging in tunnel drainage system to ensure the safety and stability of lining structure during tunnel operation. Based on the macro force and displacement characteristics of villus, the optimization of villus diameter and villus length of flocked drainage pipe at low flow rate was studied by numerical simulation. The results show that: there is a difference of 1-2 orders of magnitude between the 3-D displacements of the bottom villus and one order of magnitude between the 3-D displacements of the side villus of the flocked drainage pipe; with the increase of villus length, the 3-D displacement of villus increased parabola and with the increase of villus diameter, the 3-D displacement of villus decreased gradually; the results show that the first and third principal stresses of the bottom villus increase linearly with the increase of villus length, while the first and third principal stresses of the side villus increase parabola with the increase of villus length; when the flow rate is 2 cm/s, the diameter of villus is 0.6 mm and the length of villus is 20 mm.*

*Flocking drainage pipe anti crystal plugging technology fills the blank of tunnel drainage pipe anti crystal plugging research. This technology can reduce the maintenance cost of tunnel drainage system during operation, and ensure the safe and normal operation of the tunnel.*

Keywords*: tunnel, crystal plugging, flocking drainage pipe, Villus, principal stress, 3-D displacement*

## Introduction

By the end of 2019's, there were 19067 highway tunnels operating on the Chinese mainland, including 1175 super long tunnels and 4784 long tunnels. In the process of tunnel operation, various types of problems gradually appear, including lining leakage, fig. 1, and

---

*Corresponding author, e-mail: liushiyang@mails.cqjtu.edu.cn

lining cracking, fig. 2, caused by crystal plugging of the tunnel drainage system, fig. 3, in karst areas [1]. At present, in light of the problem of crystal plugging of tunnel drainage systems, only high-pressure gas (water) or excavation can be used for dredging, both of which are expensive and seriously affect the normal operation of a tunnel [2].

**Figure 1. Cracked lining**

**Figure 2. Water box at a leak in the lining**

**Figure 3. Crystal blockage of a drainage pipe**

To consider the problem of crystal clogging of tunnel drainage systems, this study focused on crystal composition analysis, analysis of the factors influencing the crystals, and crystal prevention and treatment techniques. The main component of the crystals in tunnel drainage pipes is insoluble calcium carbonate [3-5], and the calcium in the crystals comes mainly from the underground water [3, 6] and the cement in the shotcrete [7]. The main factors influencing crystallization plugging include the $CO_2$ partial pressure, flow rate, temperature, pH value, ion species, and concentration [8, 9]. The amount of crystallization in the drainage pipe increases with increasing pH value, and the calcium carbonate crystals are spindle shaped. The larger the pH value is, the smaller the grain size is, the more uniform the grain size is, and the more compact the accumulation is [10]. Hydrophobic treatment of the concrete base and the polyvinyl chloride pipe wall with protective coating can reduce the adhesion of calcium carbonate crystals [11, 12]. By optimizing the concrete materials and the mixtures proportions, reducing the contact between the groundwater and concrete, preventing $CO_2$ from entering the tunnel drainage pipe, adding appropriate amounts of fly ash to the shotcrete, and taking other measures, the formation of crystals can be effectively reduced [9, 13]. The crystals in drainage pipes are mainly insoluble calcite, and the phase transition from aragonite to calcite can be prevented by triblock copolymers, PEG-b-PAA-b-PS – poly (ethylene glycol)-block-poly (acrylic acid)-block-poly (styrene), [14, 15]. In the presence of biopolymers, the relative vaterite content increases with the application of ultrasonic treatment [16]. Ultrasonic treatment makes the aggregated calcium carbonate crystals more brittle [17]. The crystal structure of the calcium carbonate is changed from calcite to aragonite by green corrosion inhibitor RS1600 [18]. The cleaning solvents of single-molecule carboxylic acid organic acid reagent and polymeric carboxylic acid organic acid reagent with concentrations of 2000 ppm and dichromate indexes of 17.71% can effectively remove karst crystals from drainage systems on the premise of ensuring green environmental protection [19]. Based on the natural phenomenon, Liu *et al*. [20-24] put forward the technology of flocking drainage pipe to prevent crystal clogging from the structure of drainage pipe. At the same time, a large number of indoor tests and numerical simulation were carried out, and some useful results were obtained [25].

These studies have promoted research on the crystal blockage problem in tunnel drainage systems. In order to further study the anti-crystallization mechanism of flocked drainage pipe, this paper takes the stress and displacement characteristics of villus on the wall of flocked drainage pipe under the action of groundwater as the control standard, and analyzes the stress and displacement characteristics of typical villus on the bottom and side of flocked drainage pipe when the groundwater flow rate in the drainage pipe is 2 cm/s by using ANSYS fluid structure coupling software. At the same time, the diameter and length of villus are analyzed. The flocking parameters of villus drainage pipe were optimized by numerical simulation.

## Numerical simulation

In the numerical simulation, three kinds of villus diameter (0.6 mm, 1.0 mm, and 1.4 mm) and four kinds of villus length (5 mm, 10 mm, 15 mm, and 20 mm) were set. Combined with the field investigation results, the flow rate of 2 cm/s [22, 23] was set, and the villus was distributed at the bottom and side of the drainage pipe. The villus parameters of the drainage pipe were optimized from two aspects of stress and displacement by using ANSYS fluid structure coupling calculation module.

The ANSYS fluid structure coupling analysis steps are as follows:

- Fluid-flow (fluent) and static structural module are interrelated, mainly for the calculation of geometric model and calculation results.
- Geometric modeling (Design) [26].
- Mesh generation of geometric model.
- Flow field analysis and calculation (including velocity setting, boundary condition setting, and calculation model setting, *etc*.).
- Mesh generation of solid structure (villus).
- Boundary condition setting of solid structure, mainly setting fixed constraint at the bottom of villus.
- Import flow field calculation results (mainly pressure exerted by flow field) for calculation.
- Export calculation results. The calculation results are as follows.

## Results and discussion

### *Analysis of force and displacement characteristics of typical villus*

Two typical positions of villus at the bottom, fig. 4(a) and side fig. 4(b), of drainage pipe were selected for analysis. The diameter of villus was 0.6 mm and the length of villus was 5 mm.

Figure 5 is the 3-D displacement nephogram of the villus at the bottom of the flocking drainage pipe. It can be seen from the nephogram that:

- The maximum displacement of the villus in the X-direction is $3.6693 \cdot 10^{-14}$ m, which is distributed at the side of the villus bottom and overlaps with the peak along the villus length direction; the maximum displacement of the villus in the Y-direction is $1.7528 \cdot 10^{-12}$ m, which is mainly distributed at the upstream side of the villus top, and the cross-section is cut into three sections along the villus length direction according to the velocity; the maximum displacement in Z-direction of villi is $2.1425 \cdot 10^{-11}$ m, which is mainly distributed at the top of the villi; along the length direction, the velocity region is cylindrical with different lengths.

– The spatial displacement is mainly in Z-direction, that is, in the process of groundwater flow, the displacement of villus along the flow direction is the main control displacement, and the displacement in X-direction perpendicular to the groundwater flow direction is the smallest.

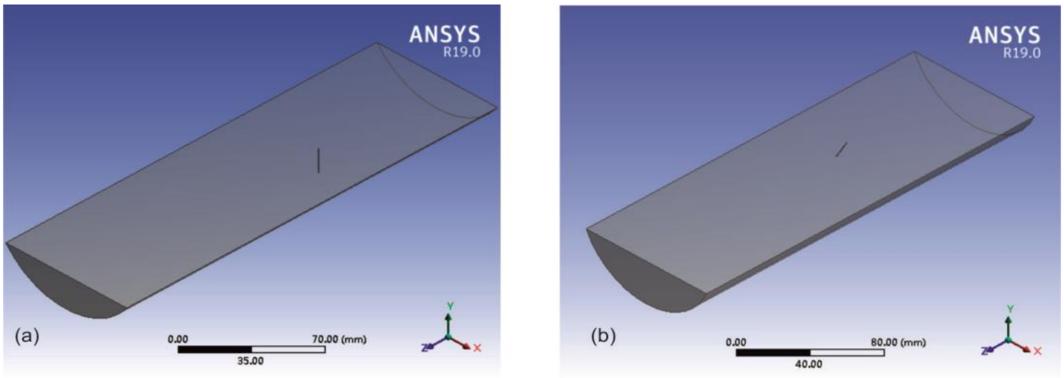


**Figure 4. Villus position of flocked drainage pipe; (a) bottom and (b) side**

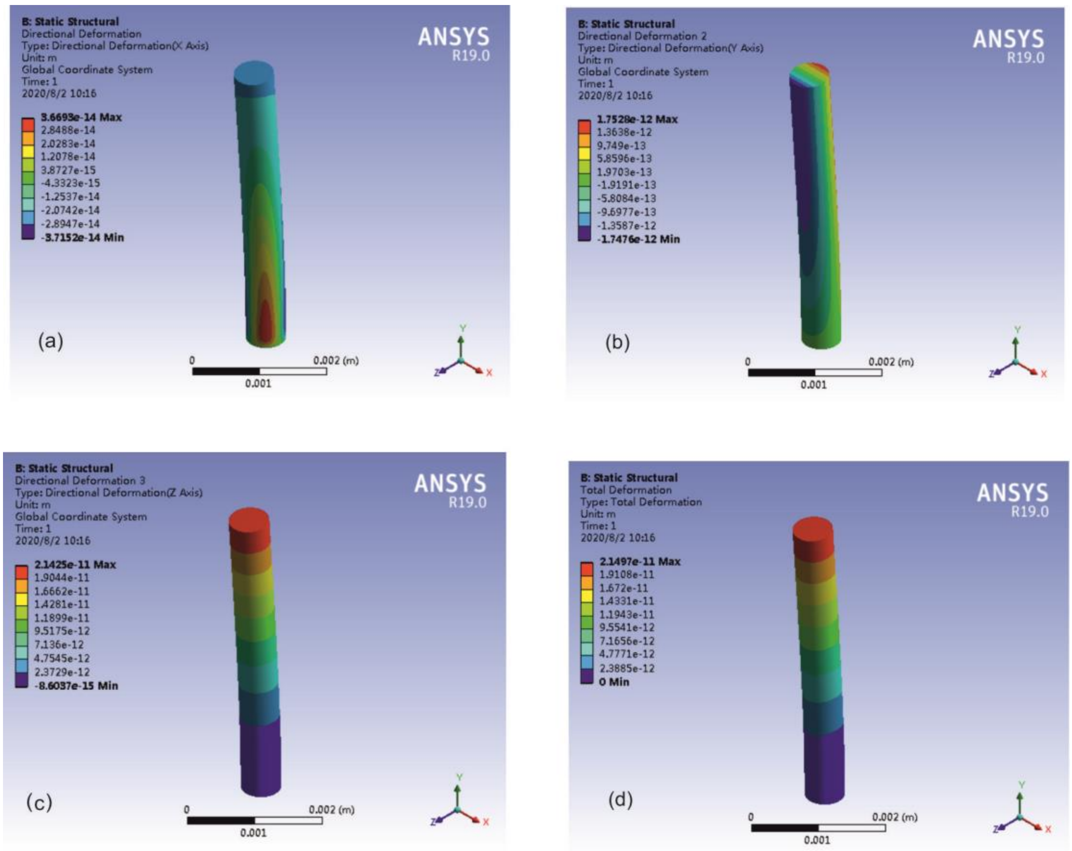


**Figure 5. Cloud chart of villus displacement at the bottom of flocking drainage pipe; (a) displacement in X-direction, (b) displacement in Y-direction, (c) displacement in Z-direction, and (d) the 3-D displacement**

Figure 6 is the stress nephogram of the villus on the side of the flocked drainage pipe. It can be seen from the graph that the first principal stress of the villus is 1025.1 Pa, and the third principal stress is –1032 Pa. The maximum stress occurs on the upstream and downstream side of the villus along the water flow direction in the drainage pipe.

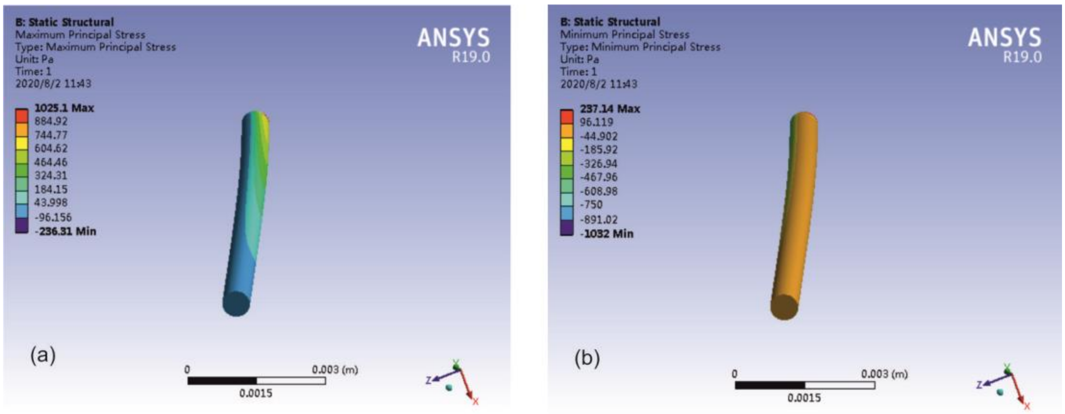


**Figure 6. Nephogram of principal stress of villus on the side of drainage pipe; (a) first principal stress of villus and (b) third principal stress of villus**

## *Optimization analysis of force and displacement of villus*

Figure 7 is the curve of the three-way displacement of the villus at the bottom of the flocking drainage pipe with the villus length. It can be seen from the figure that:
- Under different diameters, the X-direction displacement of the villus suddenly increases with the villus diameter when the villus length is greater than 15 mm, and the mutation of the villus with the diameter of 0.6 mm is the largest, and the mutation of the villus with the diameter of 1.4 mm is the smallest.
- The Y-direction displacement of villi increased gradually with the increase of villi diameter in different diameters; the increase rate of villi with diameter of 0.6 mm increased when the length was more than 10 mm, and the villi with diameter of 1.0 mm and 1.4 mm still increased slowly.
- Under different diameters, the Z-direction displacement of villi gradually increased with the increase of villi diameter; the increase rate of villi with diameter of 0.6 mm became larger when the length was greater than 10 mm, and increased in a smooth parabola; the villi with diameter of 1.0 mm and 1.4 mm still increased slowly.
- With the increase of villus diameter, the 3-D displacement of villus decreased gradually.

Figure 8 is the curve of three-way displacement of villus on the side of flocking drainage pipe with the change of villus length. It can be seen from the figure that:
- Under different diameters, the three-way displacement of villus gradually increases with the increase of villus diameter, in which the villus with diameter of 0.6 mm changes in a smooth parabola, and the villus with diameter of 1.0 mm and 1.4 mm increases slowly.
- With the increase of villus diameter, the 3-D displacement of villus decreased gradually; the 3-D displacement of villus with diameter of 0.6 mm was about 2-10 times of that of villus with diameter of 1.0 mm and 1.4 mm.

Figure 9 is the curve of the force on the bottom villi of the flocking drainage pipe changing with the length of the villi. It can be seen from the figure that with the increase of the length of the villi, the first and third principal stresses of the villi all change linearly, and the change slope when the diameter of the villi is less than 10 mm is less than that when the diameter of the villi is more than 10 mm. When the villus diameter is 0.6 mm, the first and third principal stresses are about 3-5 times of those when the villus diameter is 1.0 mm and 1.4 mm. The curves of the first and third principal stresses are approximately mirror images.

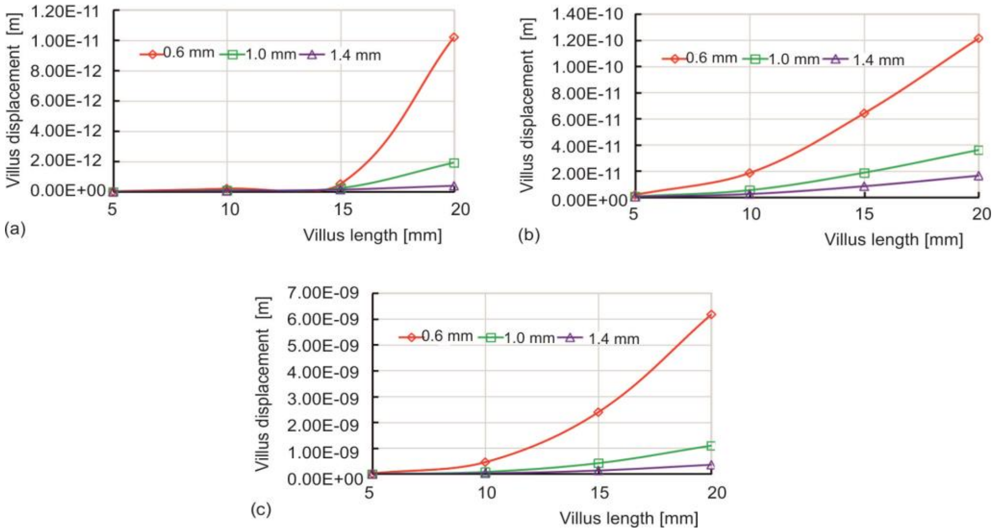


**Figure 7. Variation trend of 3-D displacement of villus at the bottom of flocked drainage pipe with villus length; (a) displacement in X-direction, (b) displacement in Y-direction, and (c) displacement in Z-direction**

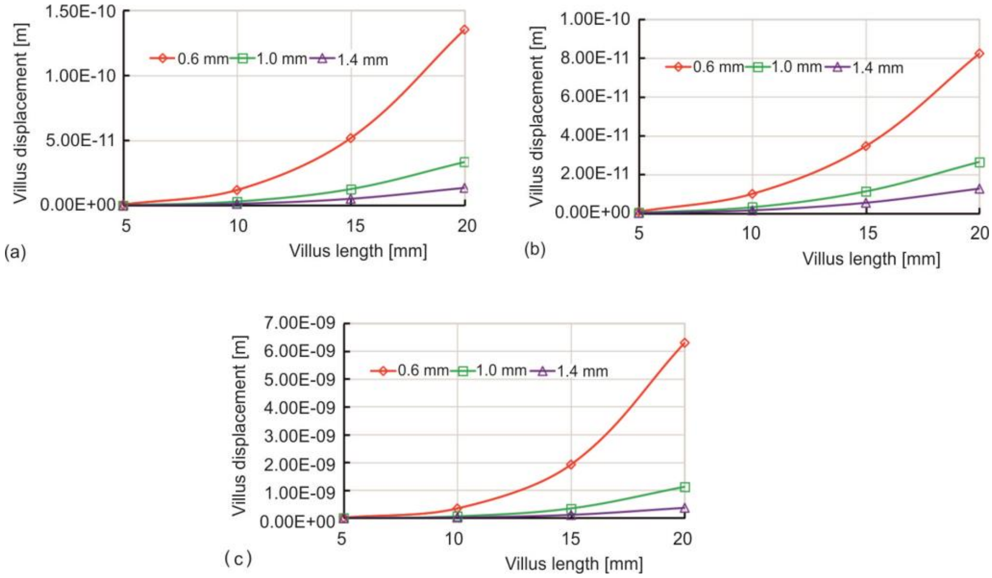


**Figure 8. Variation trend of three direction displacement of side villus of flocked drainage pipe with villus length; (a) displacement in X-direction, (b) displacement in Y-direction, and (c) displacement in Z-direction**

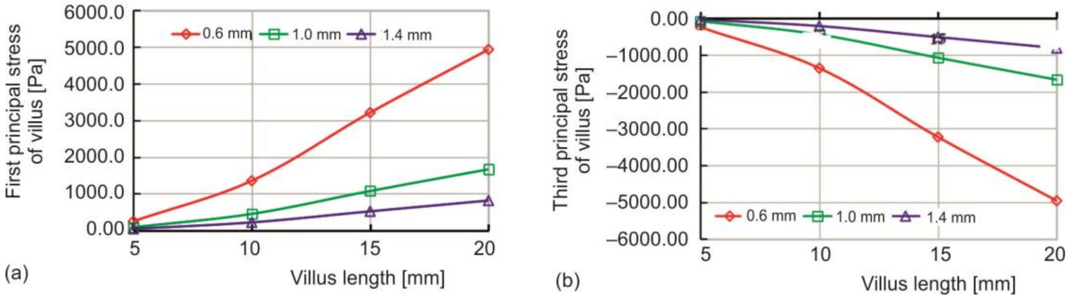

**Figure 9. Nephogram of principal stress of villus at the bottom of drainage pipe; (a) first principal stress of villus and (b) third principal stress of villus**

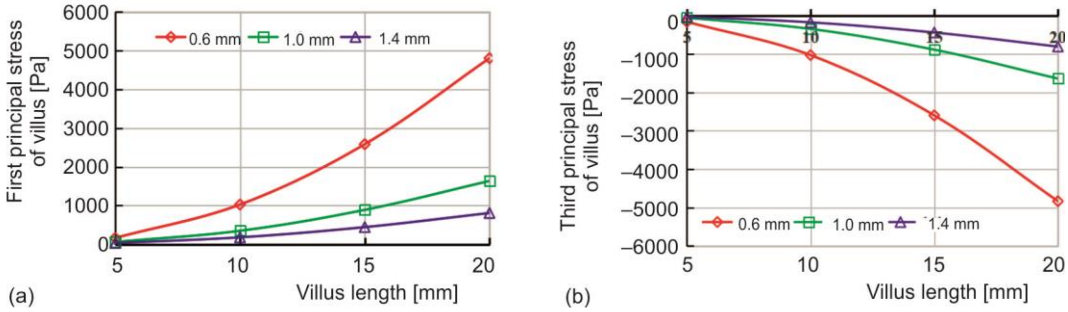

**Figure 10. Nephogram of principal stress of villus on the side of drainage pipe; (a) first principal stress of villus and (b) third principal stress of villus**

Figure 10 is the curve of the force on the side villus of the flocked drainage pipe changing with the villus length. It can be seen from the figure that with the increase of the villus length, the first and third principal stresses of the villus increase approximately in a parabola. When the villus diameter is 0.6 mm, the first and third principal stresses are about 3-5 times of those when the villus diameter is 1.0 mm and 1.4 mm. The curves of the first and third principal stresses are approximately mirror images.

## Conclusions

- The results show that there is a difference of 1-2 orders of magnitude between the 3-D displacements of the villus at the bottom of the flocked drainage pipe and 1 order of magnitude between the 3-D displacements of the villus at the side. The Z-direction displacement along the water flow direction in the drainage pipe is the largest, which is the main control displacement and occurs at the top of the villus. With the increase of villus length, the 3-D displacement of villus increased in parabola. With the increase of villus diameter, the 3-D displacement of villus decreased gradually.
- The results show that the first and third principal stresses of the bottom pile increase linearly with the increase of pile length, and the principal stresses of the side pile increase parabola with the increase of pile length. The maximum principal stress occurs at the position where the bottom of fluff contacts with the pipe wall, and distributes along the upstream and downstream sides of the water flow in the drainage pipe. With the increase of villus diameter, the first principal stress decreases and the third principal stress increases.
- To sum up, based on the macro force and displacement characteristics of villus, when the flow rate is 2 cm/s, the villus diameter of 0.6 mm and villus length of 20 mm are the best parameters for flocking drainage pipe.

## Acknowledgment

The authors show great appreciation for the financial support from the National Natural Science Foundation of China (Grant No. 51778095), the Scientific Research Project of Emei Hanyuan Expressway Project (Grant No. LH-HT-45), and the Science and technology project of Guizhou Provincial Department of transportation (Grant No. 2017-123-011).

## References

[1] Duan, H., *et al*., The Phenomenon of Crystal Pipe Blocking in Karst Tunnel and Its Induced Risk, *China Civil Engineering Journal, 53* (2020), S1, pp. 332-335
[2] Zhao, P., *et al*., Research and Application of Dredge Equipment for Drainage Pipeline in Railway Tunnel, *Railway Engineering, 58* (2018), 1, pp. 30-32+66
[3] Zhang, X., *et al*., Investigation and Analysis on Crystallization of Tunnel Drainage Pipes in Chongqing, *Advances in Materials Science and Engineering, 2018* (2018), ID7042693
[4] Guo, X., Crystallization Mechanism and Countermeasures of Drainage System for Railway Tunnel, *China Railway Science, 41* (2020), 1, pp. 71-77
[5] Lei, L., *et al*., Analysis and Treatment of Blind Pipe Blockage in Humaling Tunnel on Lanzhou-Chongqing Railway, *Modern Tunnelling Technology, 57* (2020), 6, pp. 149-153
[6] Wu, Y., *et al*., Study on Characteristics and Sources of Crystal Components of Leakage Water in the Loess Tunnel, *Modern Tunnelling Technology, 57* (2020), 6, pp. 154-159
[7] Ye, F., *et al*., Experimental Study on Scaling and Cloggingin Drainage System of Tunnels Under Construction, *China Journal of Highway and Transport, 34* (2020), 3, pp. 159-170
[8] Jiang, Y., *et al*., Investigation and Discussion on Blocking Mechanism of Drainage System in Karst Tunnels, *Railway Standard Design, 63* (2019), 7, pp. 131-135
[9] Tian, C., *et al*., Study on Mechanism of Crystal Blockage of Tunnel Drainage System and Preventive Countermeasures, *Modern Tunneling Technology, 57* (2020), 5, pp. 66-76+83
[10] Xiang, K., *et al*., Experimental Study on Crystallization Rule of Tunnel Drainpipe in Alkaline Environment, *Tunnel Construction, 39* (2019), S2, pp. 207-212
[11] Zhou, Y., *et al*., Experimental Study on Prevention of Calcium Carbonate Crystallizing in Drainage Pipe of Tunnel Engineering, *Advances in Civil Engineering, 2018* (2018), ID9430517
[12] Jiang, Y., *et al*., Experimental Research on Maintainability of Drainage Facilities in Lining Construction Joints of Karst Tunnel, *Railway Standard Design, 63* (2019), 11, pp. 91-96
[13] Ye, F., *et al*., The Disease of Scaling and Clogging in the Drainage Pipes of a Tunnel Under Construction in Yunnan, *China Civil Engineering Journal, 53* (2020), S1, pp. 336-341
[14] Su, Y., *et al*., Crystallization and Morphological Control of Calcium Carbonate by Functionalized Triblock Copolymers, *Colloids and Surfaces A: Physicochemical and Engineering Aspects, 355* (2010), 1-3, pp. 158-162
[15] Zhu, X. T., *et al*., Enhancing Performance of a GaAs/AlGaAs/GaAs Nanowire Photodetector Based on the Two-Dimensional Electron–Hole Tube Structure, *Nano Letters, 20* (2020), 4, pp. 2654-2659
[16] Kirboga, S., *et al*., The Effect of Ultrasonication on Calcium Carbonate Crystallization in the Presence of Biopolymer, *Journal of Crystal Growth, 401* (2014), Sept., pp. 266-270
[17] Su, M., *et al*., Ultrasonic Crystallization of Calcium Carbonate in Presence of Seawater Ions, *Desalination, 369* (2015), Aug., pp. 85-90
[18] Menzri, R., *et al*., Calcium Carbonate Inhibition by Green Inhibitors: Thiamine and Pyridoxine, *Desalination the International Journal on the Science & Technology of Desalting & Water Purification, 404* (2017), Feb., pp. 147-154
[19] Hong, Y., *et al*., On Scavenging Performances of Cleaning Solvents for the Clogging in the Drainage System of Karst Tunnels, *Modern Tunneling Technology, 57* (2020), 6, pp. 160-170
[20] Liu, S., *et al*., The Effect of Flocking PVC Pipe on the Prevention and Crystallization of Tunnel Drains, *Science Technology and Engineering, 18* (2018), 21, pp. 313-319
[21] Liu, S., *et al*., The Effect of Anti-Crystallization of Tunnel Plumage Drain Pipe Under Different Water Filling State, *Science Technology and Engineering, 18* (2018), 28, pp. 156-163
[22] Liu, S., *et al*., Effect of Villus Length on the Prevention of Crystallization of Tunnel Flocking Drainpipes, *Science Technology and Engineering, 19* (2019), 9, pp. 234-239

[23] Liu, S., *et al*., Experimental Study on Anti-Crystallization Law of Tunnel Transverse Flocking Drainpipe at Different Velocities, *Asia‑Pacific Journal of Chemical Engineering, 15* (2020), Apr., pp. 1-9
[24] Liu, S., *et al*., Two-Dimensional Flow Field Distribution Characteristics of Flocking Drainage Pipes in Tunnel, *Open Physics*, *18* (2020), 1, pp. 139-148
[25] Devaki, P., *et al.*, Wall Properties and Slip Consequences on Peristaltic Transport of a Casson Liquid in a Flexible Channel with Heat Transfer, *Applied Mathematics and Nonlinear Sciences, 3* (2018), 1, pp. 277-290
[26] Yang, C., *et al*., Energy Efficiency Modeling of Integrated Energy System in Coastal Areas, *Journal of Coastal Research, 103* (2020), sp1, pp. 995-1001

Paper submitted: March 5, 2121
Paper revised: June 12, 2021
Paper accepted: July 7, 2021